PAPER

Thermophysical properties of adsorbates with beyond-DFT accuracy from DFT data through error cancellation

Seth G. Porter [ID] and Bjarne Kreitz [ID] *

Predictive multiscale modeling of heterogeneously catalyzed reactions requires accurate enthalpies of adsorbates. These properties are typically calculated from density functional theory (DFT) using exchange–correlation functionals with the generalized-gradient approximation (GGA) since more accurate electronic structure methods are not feasible. Therefore, the derived enthalpies are subject to large inaccuracies. We address this challenge through an error-cancellation approach that builds on the connectivity-based hierarchy (CBH) to derive enthalpies of formation of adsorbates with beyond-DFT accuracy without increasing computational cost. This method constructs reactions that conserve the electronic configuration between the target and the reference species, leading to error cancellation. The method is applied to adsorbates on Pt(111), Ni(111), and MgO(100). With the CBH method, it is possible to determine enthalpies of formation that are in excellent agreement with experimental measurements for a range of adsorbates and across many GGA exchange–correlation functionals, clearly outperforming conventional referencing approaches. Additionally, the method combines available experimental surface science data with gas-phase thermochemistry data and DFT data in a global thermochemical network. More accurate enthalpies of formation have a tremendous impact on the predictive performance of multiscale models and enable more conclusive insights into reaction mechanisms of catalytic reactions.

Introduction

Accurate thermophysical properties of adsorbates are essential quantities to elucidate the reaction mechanisms of heterogeneously catalyzed reactions and to predict the performance of catalytic materials through microkinetic modeling. In a microkinetic model, the enthalpy, entropy, and heat capacity are required for each adsorbed or gas-phase species in the reaction mechanism to evaluate the Gibbs free energy, which is used to determine the equilibrium constants of each

School of Chemical and Biomolecular Engineering, Georgia Institute of Technology, Atlanta, USA. E-mail: bkreitz3@gatech.edu; Tel: +1 4048941835

elementary step.[1] Entropy and heat capacity are species-specific properties that can be obtained directly from the partition functions of each species, without knowledge of the partition functions of other species. Partition functions for adsorbates are typically calculated from the vibrational modes assuming the harmonic oscillator approximation. It is also possible to derive partition functions more accurately by accounting for anharmonicity.[2,3] In contrast, enthalpies are relative quantities that are only physically meaningful when referenced to other species. Reference species and energies can be arbitrarily defined, but the most common and widely adopted reference frame is the enthalpy of formation, in which every species is referenced to the elements in their standard states. The gas-phase community has compiled thermochemical databases, such as the Active Thermochemical Tables (ATcT)[4,5] that contain highly accurate enthalpies of formation for thousands of molecules. The construction of these thermochemical networks was made possible through the high level of theory quantum mechanical methods for molecular systems that allow the computation of reaction enthalpies with sub-kJ mol^{-1} accuracy,[6-8] extensive amounts of experimental data, and adherence to the standards of the enthalpies of formation framework.

The situation for thermophysical properties of adsorbates on catalytic surfaces is markedly different.[9] Experimental techniques to determine the thermophysical properties of adsorbates are available, such as single-crystal adsorption calorimetry or temperature-programmed desorption,[10-12] but they are challenging to perform. Therefore, the amount of experimentally determined enthalpies of formation of adsorbates on either transition metal[13,14] or metal oxide surfaces[15] is limited. This data scarcity is further complicated by the variety of active site motifs of heterogeneous catalysts and their dynamic transformation under reaction conditions.[16] Consequently, most thermophysical properties of adsorbates will never be measured and have to be determined from electronic structure calculations instead. A range of higher level of theory methods is available, including meta-GGA or hybrid functionals,[17] RPA,[18-20] CCSD(T),[21] quantum Monte Carlo,[22] and embedding techniques.[23] However, these methods are prohibitively expensive and can currently only be applied to study a few adsorbates. Therefore, DFT with GGA exchange–correlation functionals remains the only available level of theory routinely applicable for parameterizing microkinetic models or elucidating mechanisms, but DFT-derived thermophysical properties are subject to significant inaccuracies. Wellendorff et al.[24] compared a range of DFT functionals against a set of experimental adsorption enthalpies on transition metals, and they observed average deviations on the order of ± 30 kJ mol^{-1}. Additionally, there are substantial variations between different GGA exchange–correlation functionals,[24] making it difficult to choose the correct functional for a specific task. Adsorption reaction enthalpies generally have large deviations because gas-phase species are poorly described by GGA-DFT, and *ad hoc* corrections are often introduced for individual species to improve agreement with the gas-phase thermochemistry.[25-27] The large inaccuracies in energetic properties derived from GGA-DFT prevent the conclusive elucidation of reaction mechanisms or insights into the relevant pathways, and limits the predictive accuracy of multiscale models for catalytic materials.[28-32]

It is generally assumed that higher level of theory calculations are required to improve the accuracy of the computed enthalpies of formation of adsorbates. However, this is not the only path to accurate enthalpies of formation. The gas-

phase community has developed methods to improve the accuracy of thermo-physical properties derived from lower levels of theory, such as DFT or Hartree–Fock, by leveraging the concept of error cancellation.[33–37] The idea behind the error-cancellation technique is to create reactions of reference species, whose enthalpies of formation are accurately known, that preserve the bonding environment and hybridization of the target species. Since electronic structure methods make consistent errors in the fragments of the target and the reference species (for those fragments), these errors cancel out, leading to more accurate reaction enthalpies. Error cancellation for molecular systems was initially developed by Pople and co-workers[33,34] in 1970 using bond-separation (isodesmic) reactions that conserve the bond types of the target. Building on these reactions, a range of homodesmotic reaction types were developed that further increase the conservation of the target structure.[35,38] Raghavachari and co-workers[36] systemized the approach by formulating the connectivity-based hierarchy (CBH), a framework to automatically construct error-cancellation reactions by decomposing the target molecule based on its Lewis structure. CBH is a rung-based approach that increasingly conserves the structure of the target species in the references, leading to more effective error cancellation and more accurate enthalpies of formation. Through this technique, it is possible to derive enthalpies of formation of molecules from lower levels of theory with chemical accuracy (± 1 kcal mol^{-1}).[35,36,39,40] Error cancellation techniques such as the CBH method are still being actively used and developed to derive accurate enthalpies of formation for gas-phase species.[41,42] This method was extended by Kreitz et al.[43] to adsorbates, and successfully applied to derive accurate enthalpies of formation for a set of adsorbates on Pt(111) via isodesmic reactions for the first time.

In this study, we expand our previously developed error-cancellation approach to a broader set of adsorbates on transition-metal surfaces, including Pt(111) and Ni(111), and to higher CBH rungs. Additionally, we demonstrate the application of the CBH scheme to adsorbates on metal oxide surfaces, using n-alkanes on MgO(100) as a benchmark. The error-cancellation approach is combined with rigorous uncertainty quantification using the correlated uncertainty space spanned by the BEEF-vdW ensemble. Results show that the CBH method can lead to substantial error cancellation, thereby improving the accuracy of enthalpies of formation derived from GGA-DFT energies. Using the CBH approach for adsorbates, it is possible to derive enthalpies of formation of adsorbates on metal and metal oxide surfaces that surpass the limitations of DFT accuracy. These error-cancellation approaches combine experimental surface science data and DFT-derived energetics within a global thermochemical network, providing a bridge between experimental surface science and electronic structure data. More accurate thermophysical properties improve the predictions of multiscale models and aid in the conclusive elucidation of reaction mechanisms for heterogeneously catalyzed reactions.

Methods

Electronic structure theory

DFT calculations were performed with QuantumEspresso[44,45] using the BEEF-vdW exchange–correlation functional[46] and PAW pseudopotentials. The adsorbate on the Pt(111) or Ni(111) was modeled as a 4-layer slab with a 3×3 supercell using

optimized lattice constants. This configuration corresponds to an adsorbate coverage of 1/9th ML. The atomic positions of the two bottom layers were fixed. Adsorbates were relaxed until all forces were converged to within 0.025 eV Å^{-1} with a cutoff energy of 50 Ry and a ($5 \times 5 \times 1$) k-point grid. A vacuum of 17 Å was used in combination with Marzari–Vanderbilt smearing with a width of 0.02 Ry. Single-point energies were calculated from the optimized structure with a cutoff energy of 60 Ry. DFT calculations for Ni(111) were performed with spin polarization. Further single-point energies were computed without re-optimizing the structures for a range of different GGA exchange–correlation functionals with D3 dispersion corrections[47] and without such corrections, including PBE, RPBE, PW91, revPBE, RPBE+D3, PBE+D3, revPBE+D3, and PBEsol+D3.

Geometry optimizations for the adsorbates on MgO(100) were similarly performed with the BEEF-vdW functional using an optimized lattice constant of 4.28 Å and a vacuum of 16 Å. A (4×4) unit cell was used to fit the larger alkanes, and calculations were performed using the Γ-point. Electron smearing was done with the Marzari–Vanderbilt method and set to 0.02 Ry width. The structures were converged to below 0.025 eV Å^{-1}. Structure optimizations for gas-phase species were performed in a box of $(20 \text{ Å})^3$ at the Γ-point. Raw DFT results and structures are listed in the supplementary information (SI).

Conventional approach to derive enthalpies of formation *via* adsorption reactions

To derive enthalpies of formation of the adsorbed species, it is necessary to anchor the adsorbates to the existing gas-phase thermochemical network. In this study, we use the Active Thermochemical Tables[4,5] as the global thermochemical network. The most common approach to derive the enthalpies of formation of adsorbates is to construct a hypothetical reaction of gas-phase species and a vacant surface site to form the adsorbed species.[9,48,49] Typical choices for reference species are CH_4, H_2O, and H_2 for $C_xH_yO_z$* adsorbates,[9,48] but other choices are possible. The only restriction is that the enthalpy of formation of the reference species needs to be known and that one gas-phase species is chosen per element. Fig. 1a shows the adsorption reaction to derive the enthalpy of formation of monodentate formate, along with the thermochemical cycle to determine the enthalpy of formation. The enthalpy of this adsorption reaction is determined from the zero-point corrected DFT energies $\Delta_r H^{QM}$. In combination with the known enthalpies of formation of the gas-phase reference species, the enthalpy of formation of the target $\Delta_f H_{P*}$ can be determined *via* eqn (1).[9]

$$\underbrace{\Delta_f H_{P*}}_{\text{target}} = \Delta_r H^{QM} - \sum_{i \neq P*}^{N} \nu_i \Delta_f H_i = \underbrace{E_{P*}}_{\text{target}} + \underbrace{\sum_{i \neq P*}^{N} \nu_i E_i}_{\text{references}} - \underbrace{\sum_{i \neq P*}^{N} \nu_i \Delta_f H_i}_{\text{references}} \quad (1)$$

Connectivity-based hierarchy for adsorbates

The connectivity-based hierarchy is a method to systematically create hypothetical reactions of reference species that conserve the bonding environment and hybridization of the target to maximize error cancellation, leading to more accurate $\Delta_r H^{QM}$. Ramabhadran and Raghavachari[36] developed the CBH method
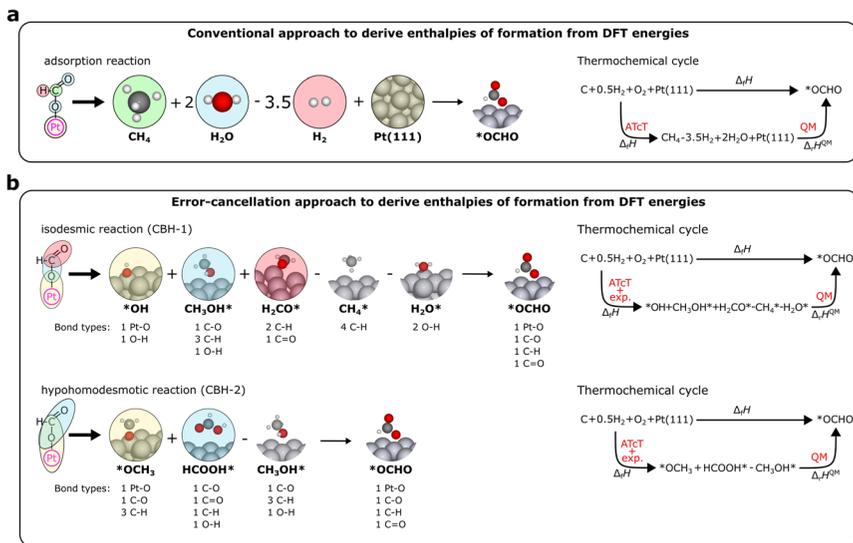
Fig. 1 (a) Conventional adsorption reaction approach to determine the enthalpy of formation of monodentate formate *OCHO on Pt(111) from DFT data. (b) Error-cancellation approach of the connectivity-based hierarchy to determine the enthalpy of formation of *OCHO via the CBH-1 (isodesmic reaction) and CBH-2 (conservation of the immediate connectivity of heavy atoms) reaction. The colored ellipses highlight the decomposition of the target into the heavy atoms (adsorption reaction approach), or the bond-type fragments (CBH-1&2). Additional species are required to balance the stoichiometry. The thermochemical cycle illustrates how the enthalpies of formation of the reference species are determined and how the enthalpy of formation of *OCHO is derived from the reference species. Bond types of each species are listed in (b) to demonstrate their conservation.

for closed-shell organic molecules, but it has been extended to other systems.[39,40,50–52] The CBH method is a rung-based approach that alternates between atom-centric and bond-centric conservation reactions, expressed as CBH-n, with $n = 0, 1, 2$, etc. Higher rungs conserve larger features of the target species and lead to higher degrees of error cancellation, providing a hierarchy for the referencing reactions. In the CBH method, the target species is separated into fragments, which define the reference species, and the rung of the CBH scheme defines the size of the fragments. At CBH-0, the species is separated into the heavy (non-hydrogen) atoms, and all broken bonds are hydrogenated to create an isogyric reaction that conserves the spin pairs. The CBH-1 scheme creates an isodesmic reaction, in which the species is separated into its various covalent bonds. Higher rungs are isodesmic-type reactions that also conserve the immediate connectivity of every heavy atom (hypohomodesmotic reaction, CBH-2) or the immediate connectivity of every bond (hyperhomodesmotic reaction, CBH-3). Further rungs are possible but not of practical relevance due to the limitations of highly accurate thermophysical data for large reference species. Additionally, CBH-1 to CBH-3 rungs are typically sufficient to achieve chemical accuracy.[36,37,41] By following a set of rules in creating these reactions (e.g., consideration of end or branching points in the molecule), an automated framework was developed to

construct these error-cancellation reactions using only the Lewis structure of the target for molecules of arbitrary complexity.[36]

The CBH method was extended to adsorbed species by Kreitz et al.,[43] and a detailed description of the CBH method for adsorbates is provided in ref. 43. It can be applied to all adsorbates, including physisorbed, monodentate, or multidentate species. Fig. 1b shows exemplarily the referencing reactions at the CBH-1 and CBH-2 level for monodentate formate (*OCHO). The CBH-0 level is omitted, because there is almost no error cancellation and inconsistencies can occur.[43] These inconsistencies are prevented using the isodesmic reactions of the higher rungs. Similar to the molecular systems, the adsorbate is separated into the various bond types according to its Lewis structure. Monodentate formate can be separated into a Pt–O, C–O, and C=O bond (bonds to H are not considered in the CBH scheme), which requires *OH (Pt–O), CH_3OH* (C–O), and H_2CO* (C=O) as reference species at the isodesmic reaction of the CBH-1 level. An assumption is that the reference species for the bond types that do not directly involve a covalent bond to the surface are represented as physisorbed species instead of gas-phase molecules. Since the entire target adsorbate interacts via dispersion with the catalyst surface, the usage of physisorbed species leads to a better conservation of the electronic configuration. In this case, CH_4^* and H_2O* are required to balance the stoichiometry since the C and O atoms are counted twice (see Fig. 1). This isodesmic reaction conserves all the bond types in monodentate formate, including C–H bonds. At the CBH-2 level, the target is broken down into a PtOC and O–C=O fragment for which methoxy (*OCH_3) and formic acid (HC(O)OH*) are used as reference species, along with CH_3OH* to balance the stoichiometry. The various rungs on the ladder are connected; products from lower rungs become the reactants on higher rungs.[36]

A software package is available that can automatically construct the error cancellation reactions for adsorbates based on the SMILES string.[42,43] No extensions or modifications of the adsorbate CBH method are required to use it for Ni(111) or for the MgO(100) facet. To determine the enthalpy of formation of a target P* (here *OCHO), we use the thermochemical cycle shown in Fig. 1b. Calculation of the enthalpies of formation of the adsorbates using the, e.g., isodesmic or homodesmotic reactions is similar to the adsorption reaction method (see eqn (2)); the only difference is the choice of reference species. Enthalpies of formation of the reference species, here adsorbates instead of gas-phase species, need to be known from either experiments or higher level of theory calculations. For the presented benchmark species in this work, we rely on experimental adsorption enthalpies to determine the enthalpies of formation of the reference adsorbates in combination with the known enthalpy of formation of the gas-phase precursor. The reaction enthalpy $\Delta_r H^{QM}$ to form the target from the reference species is derived from zero-point corrected DFT energies according to the reaction of the CBH rung. With the known enthalpies of formation of the reference species $\Delta_f H_i$, it is possible to back out the enthalpy of formation of the target $\Delta_f H_{P*}$ via eqn (2).

$$\underbrace{\Delta_f H_{P*}}_{\text{target}} = \Delta_r H^{QM} - \underbrace{\sum_{i \neq P*}^{N} \nu_i \Delta_f H_i}_{\text{references}} = \underbrace{E_{P*}}_{\text{target}} + \underbrace{\sum_{i \neq P*}^{N} \nu_i E_i}_{\text{references}} - \underbrace{\sum_{i \neq P*}^{N} \nu_i \Delta_f H_i}_{\text{references}} \qquad (2)$$

Enthalpies of formation of reference and benchmark species

Enthalpies of formation of the gas-phase species that were used as references for the adsorption reaction approach were taken from the Active Thermochemical Tables[5] (version 1.220) and are listed in Table 1.

The enthalpies of formation of the adsorbates for the CBH approach were derived from experimental surface science measurements over single-crystal surfaces obtained from the literature in combination with accurate gas-phase enthalpies of formation. Temperature corrections were applied to evaluate the enthalpies of formation of the adsorbates at the temperatures of the experiments and to convert the enthalpies of formation to 0 K. These temperature corrections are based on accurate NASA polynomials of the gas-phase species and for adsorbates we used the vibrational modes to derive partition functions assuming the harmonic oscillator model with in-house routines. The procedure is outlined in detail in Section 1 of the SI. Enthalpies of formation of the reference species that are used for the isodesmic reactions on Pt(111) are reported in ref. 43 and provided in Table S2. Table 2 shows the derived enthalpies of formation of the benchmark species for Pt(111) and Ni(111) as well as the reference species for Ni(111). The values for methoxy on Pt(111) and Ni(111) were corrected from the original studies because the experimental values are reported at a high coverage.[53,54] We used the measured coverage-dependent heat of adsorption and integrated up to a total coverage (methoxy and hydroxyl) of 1/9 ML to achieve a fairer comparison between experiments and theory (see SI).

The derivation of the enthalpies of formation of the physisorbed n-alkanes on MgO(100) is similar to the procedure for the adsorbates on the transition metal surface. However, an issue for metal oxide surfaces is the enthalpy of formation of the vacant surface site. For transition metal surfaces, we typically define the Pt(111) or Ni(111) surface to correspond to bulk Pt or Ni, leading to enthalpies of formation of 0 kJ mol^{-1}.[9] MgO(100) would be referenced to Mg and O$_2$ in their standard state, but the reaction enthalpy to form the surface from the elements is not accurately known and cannot be accurately computed from DFT. Therefore,

Table 1 Enthalpies of formation of the gas-phase species at 298.15 K from the Active Thermochemical Tables, version 1.220 (ref. 5)

Species	$\Delta_f H_{298K}$ (kJ mol^{-1})	Uncertainty (kJ mol^{-1})
H$_2$(g)	0	Exact
O$_2$(g)	0	Exact
CH$_4$(g)	−74.513	±0.043
CH$_3$OH(g)	−200.85	±0.14
HC(O)OH(g)	−378.28	±0.20
C$_2$H$_6$(g)	−84.02	±0.12
H$_2$O(g)	−241.808	±0.022
C$_3$H$_8$(g)	−105.00	±0.15
n-C$_4$H$_{10}$(g)	−125.55	±0.18
n-C$_6$H$_{14}$(g)	−166.77	±0.32
n-C$_8$H$_{18}$(g)	−207.89	±0.51

Table 2 Measured heats of adsorption on Pt(111) and Ni(111), and derived enthalpies of formation at 0 K for the benchmark species and those that were used as fragments for the error-cancellation reactions. All enthalpies are in kJ mol^{-1}

Species	Reaction	ΔH_{ads}	T (K)	$\Delta_f H_{0\,K}^{exp}$	Ref.
n-C$_4$H$_{10}^{*}$	n-C$_4$H$_{10}$(g) + Pt(111) $\rightleftharpoons$ n-C$_4$H$_{10}$/Pt(111)	-51	171	-151	55
*OCH$_3$	CH$_3$OH(g) + /Pt(111) $\rightleftharpoons$ OCH$_3$/Pt(111) + OH/Pt(111)	-74	150	-161	53
HC(O)OH*	HC(O)OH(g) + /Pt(111) $\rightleftharpoons$ HC(O)OH/Pt(111)	-58	100	-429	56
C$_3$H$_8^{*}$	C$_3$H$_8$(g) + /Pt(111) $\rightleftharpoons$ C$_3$H$_8$/Pt(111)	-41	139	-123	55
*OCHO^{a,b}	HC(O)OH(g) + O/Pt(111) $\rightleftharpoons$ OCHO/Pt(111) + OH/Pt(111)	-78	130	-357	56
CH$_3$OH*	CH$_3$OH(g) + Ni(111) $\rightleftharpoons$ CH$_3$OH/Ni(111)	-60	100	-248	54
D$_2$O*	D$_2$O(g) + Ni(111) $\rightleftharpoons$ D$_2$O/Ni(111)	-54	100	-291	57
*OD	D$_2$O(g) + O/Ni(111) $\rightleftharpoons$ 2 OD/Ni(111)	-67	170	-270	57
*O	O$_2$(g) + 2 Ni(111) $\rightleftharpoons$ 2 O/Ni(111)	-480	300	-238	11
*OCH$_3$	CH$_3$OH(g) + O/Ni(111) $\rightleftharpoons$ OCH$_3$/Ni(111) + OH/Ni(111)	-81	100	-236	54

^{a} The measured heat of adsorption of these reactions was corrected by 2 kJ mol^{-1} compared to the original paper due to a systematic error as described in ref. 13. ^{b} The experimental heat of reaction was obtained at a coverage of 1/4 ML. The enthalpy of formation was corrected by 10 kJ mol^{-1} with the relation provided in ref. 56.

enthalpies of formation of adsorbates on metal oxide surfaces are typically not calculated or reported in the literature.[15] For our purposes, the actual value of the MgO(100) surface does not matter since the experimental and DFT-derived enthalpies of formation of the adsorbates are referenced to the same enthalpy of formation value for MgO(100). Consequently, we decided to set the enthalpy of formation of MgO(100) to $\Delta_f H_{MgO(100)} = 0$ kJ mol^{-1}. Experimental enthalpies of formation of the alkanes on MgO(100) using the definition for MgO(100) are summarized in Table 3.

Table 3 Experimental heats of adsorption of alkanes on MgO(100) determined from temperature-programmed desorption and derived enthalpies of formation at 0 K. All enthalpies are in kJ mol^{-1}

Species	Bond type	Reaction	ΔH_{ads}	T (K)	$\Delta_f H_{0\,K}^{exp\,a}$	Ref.
CH$_4^{*}$	C–H	CH$_4$(g) + MgO(100) $\rightleftharpoons$ CH$_4$/MgO(100)	-12.3	47	-76	12
C$_2$H$_6^{*}$	C–C	C$_2$H$_6$(g) + MgO(100) $\rightleftharpoons$ C$_2$H$_6$/MgO(100)	-22.5	75	-90	12
C$_3$H$_8^{*}$	C–C–C	C$_3$H$_8$(g) + MgO(100) $\rightleftharpoons$ C$_3$H$_8$/MgO(100)	-29.4	93	-112	12
n-C$_4$H$_{10}^{*}$	C–C–C–C	n-C$_4$H$_{10}$(g) + MgO(100) $\rightleftharpoons$ n-C$_4$H$_{10}$/MgO(100)	-35.4	111	-137	58
n-C$_6$H$_{14}^{*}$	N/A	n-C$_6$H$_{14}$(g) + MgO(100) $\rightleftharpoons$ n-C$_6$H$_{14}$/MgO(100)	-47.0	144	-182	12
n-C$_8$H$_{18}^{*}$	N/A	n-C$_8$H$_{18}$(g) + MgO(100) $\rightleftharpoons$ n-C$_8$H$_{18}$/MgO(100)	-63.6	175	-234	12

^{a} We assumed that the enthalpy of formation of MgO(100) is 0 kJ mol^{-1}.

Results

CBH for adsorbates on transition metal surfaces

The CBH method is applied to adsorbates listed in Table 2 for which experimental enthalpies of formation are available to benchmark its accuracy. All DFT data and scripts are provided in ref. 59. Depending on the size and structure of the molecule, it may be possible to use only the isodesmic reaction (CBH-1) or to climb to higher rungs on the CBH ladder. Fig. 2 displays the deviation of the computed enthalpy of formation from the experimental value for both the conventional adsorption reaction approach and the CBH scheme for selected adsorbates on the transition metal surfaces, evaluated with various GGA exchange–correlation functionals. The experimental enthalpy of formation of n-C_4H_{10}/Pt(111) is -151 kJ mol^{-1} and the value derived from the BEEF-vdW functional using the adsorption reaction approach is in good agreement with the experimental value. All other GGA functionals deviate significantly from the experiments, especially if dispersion is not considered (see Fig. 2a). BEEF-vdW gives the best result for the conventional referencing approach *via* the adsorption reaction, because it is a semi-empirical functional that was fitted to experimental adsorption energies.[46] When using the isodesmic reactions (CBH-1) to derive the enthalpy of formation, the agreement with the experimental value improves drastically across all functionals, *e.g.* the error for the RPBE functional is reduced by more than 50 kJ mol^{-1}. Computed enthalpies of formation of each functional are within the experimental accuracy of ± 10 kJ mol^{-1}.[10] Climbing to CBH-2 improves the agreement further for most functionals, but there is a slightly larger deviation from the experimental value for BEEF-vdW and PBE/D3. The homodesmotic reactions predict a more negative enthalpy of formation of butane, corresponding to a stronger adsorption of butane on Pt(111). The experimental value reported here is determined at a butane coverage of 1/3 ML,[55] whereas the DFT calculations are performed at a low coverage of 1/9 ML. When
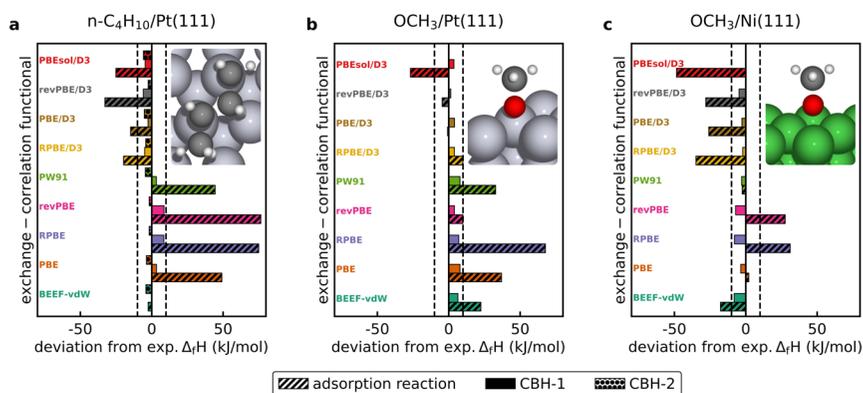

Fig. 2 Comparison of computed and experimental enthalpies of formation of (a) n-$C_4H_{10}^*$ on Pt(111), (b) *OCH$_3$ on Pt(111), and (c) *OCH$_3$ on Ni(111) using the conventional adsorption reaction approach and the error cancellation reactions of the connectivity-based hierarchy. Experimental enthalpies of adsorption are reported in Table 2 and the dashed lines represent the experimental accuracy of ± 10 kJ mol^{-1}.

performing a DFT calculation for a higher butane coverage of 2/9 ML (2 butane molecules per 3 × 3 unit cell), the enthalpy of formation is less negative by 2 kJ mol^{-1}. This shift indicates a small destabilization and could lead to a better agreement with the predictions of the CBH-2 rung.

An experimental enthalpy of formation of -161 kJ mol^{-1} is determined for methoxy on Pt(111) (see Fig. 2b). The enthalpy of formation derived using the adsorption reaction method with the BEEF-vdW energies results in a deviation of 23 kJ mol^{-1}, whereas the isodesmic reaction predicts a more accurate enthalpy of formation of -164 kJ mol^{-1}. Similar results are obtained for methoxy on Ni(111) (see Fig. 2c), which has an experimental enthalpy of formation of -236 kJ mol^{-1}, where the value from the isodesmic reaction is -244 kJ mol^{-1} and the adsorption approach leads to -254 kJ mol^{-1}. The results from the adsorption reaction approach also vary substantially between the functionals and deviate from the experimental value. With the isodesmic reaction, the enthalpies of formation predicted by all GGA exchange–correlation functionals are within ±8 kJ mol^{-1} for both transition metal surfaces. Thus, the isodesmic reactions demonstrate a reduction in the individual functional errors of more than 50 kJ mol^{-1}, without the use of higher level of theory calculations, *ad hoc* corrections to specific species, or an increase in computational cost. From this benchmark, it is possible to conclude that the isodesmic or homodesmotic referencing reactions almost completely remove the dependence of the GGA functional on the enthalpy of formation.

The BEEF-vdW functional provides a way to determine the computational uncertainty of the DFT energy, when using a semi-empirical functional. After the self-consistent field calculation, a non-self-consistent field calculation is performed where the exchange-enhancement factor is perturbed according to the Bayesian error estimate from the training of the functional.[46] This ensemble of energies can be propagated through either the adsorption reaction or the CBH approach to estimate the uncertainty in the derived enthalpy of formation, while accounting for correlations among the various species. The violin plots in Fig. 3 show the density distribution of the enthalpy of formation derived from the BEEF-vdW ensemble and include results from the eight GGA exchange–correlation functionals tested in this study. BEEF uncertainty estimates of the enthalpy of formation for butane (Fig. 3a) derived with the adsorption reaction reveal a large absolute deviation of more than ±75 kJ mol^{-1} and a standard deviation of 24 kJ mol^{-1} from the experimental value. These large deviations are similar to the results from the exchange–correlation functionals in Fig. 2. Results from the exchange–correlation functionals are always within the BEEF uncertainty estimate for all species that were investigated in this study. Using an isodesmic reference reaction for butane results in a significant reduction in the uncertainty of its enthalpy of formation due to the cancellation of errors. Additionally, the probability density distribution is also more tightly clustered around the nominal value ($\sigma = 6$ kJ mol^{-1}). Climbing to the CBH-2 rung, which has an even higher degree of error cancellation, shows that all the GGA exchange–correlation functionals lead to essentially the same result. The BEEF uncertainty is further reduced to a standard deviation of $\sigma = 3$ kJ mol^{-1}.

Methoxy and propane show the same results. The isodesmic reaction leads to more accurate enthalpies of formation across the BEEF uncertainty range with standard deviations of 4 kJ mol^{-1} and 2 kJ mol^{-1}, respectively (see Fig. 3b and c).
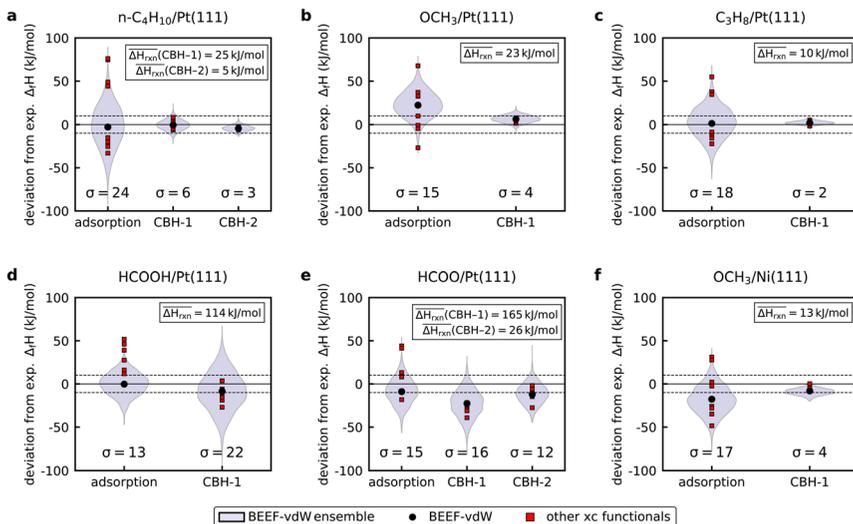
Fig. 3 Comparison of experimental enthalpy of formation of (a) n-$C_4H_{10}^*$, (b) *OCH_3, (c) $C_3H_8^*$, (d) HCOOH*, and (e) *OCHO on Pt(111) with the enthalpies of formation derived from various GGA exchange–correlation functionals and the density curves spanned by the BEEF ensemble. (f) Benchmarking of *OCH_3 on Ni(111). The experimental enthalpies of formation of the reference species were not subjected to an uncertainty. Standard deviations σ are given in kJ mol^{-1}.

Additionally, all functionals yield almost identical enthalpies of formation, which are in excellent agreement with the experimental value. Results for methoxy adsorbed on Ni(111) in Fig. 3f are similar to methoxy on Pt(111), where the isodesmic reaction leads to a drastic improvement in the enthalpy of formation and reduction in the uncertainty. The results for formic acid in Fig. 3d are less good. Using the isodesmic reaction actually leads to a larger uncertainty in the enthalpy of formation ($\sigma = 22$ kJ mol^{-1}) than the adsorption reaction approach ($\sigma = 13$ kJ mol^{-1}). The uncertainties of the enthalpies of formation for monodentate formate are similar for the adsorption reaction approach and the isodesmic reaction, although the nominal BEEF-vdW values deviate from each other. Climbing to CBH-2 improves agreement between experiments and theory and reduces uncertainty. However, the uncertainty is still on the order of 15 kJ mol^{-1}.

Fig. 3 reveals two important findings. First, the propagation of the correlated uncertainties of the BEEF-vdW functional and the reduction in the uncertainty of the enthalpy of formation from the CBH method strengthen the claim that the error cancellation reactions can lead to the same enthalpies of formation regardless of the choice of GGA functional. This finding provides further proof of the suitability of error-cancellation reactions for adsorbates. Results for n-C_4H_{10} show that climbing the CBH ladder leads to improved error cancellation due to a better conservation of the bonding environment and hybridization of the target. However, the results also show that isodesmic or hypohomodesmotic reactions created with the CBH method do not always achieve a high degree of error cancellation reactions (*i.e.* it is not guaranteed). The isodesmic reactions for formic acid and monodentate formate perform similarly or even slightly worse

compared to the conventional approach. Comparing the reaction enthalpies for these reactions shows that the reaction enthalpies are much larger for these two species than for the referencing reactions that exhibit error cancellation. The low degree of error cancellation is a result of the poor conservation of the hybridization of the C atom in formate or methoxy and formaldehyde (H$_2$CO*), which are used as the reference species. We have previously concluded that the reaction enthalpy is a good indicator for the effectiveness of the error cancellation reaction;[43] lower reaction enthalpies achieve higher degrees of error cancellation since the structure of the target is better conserved. Yet, there can be cases where the reaction enthalpy is close to 0, while the effect of error cancellation is only minor. For example, the CBH-2 reaction for formate in Fig. 3e shows this effect, making the reaction enthalpy a weak criterion. The uncertainty estimate from the BEEF ensemble provides an alternative tool for testing the effectiveness of error-cancellation reactions. A significant reduction in the uncertainty of the BEEF ensemble indicates a high degree of error cancellation. The ensembles can be obtained at almost no extra cost from the optimized adsorbate structure and, thus, provide a convenient way to assess the performance of the referencing reaction.

CBH for MgO(100)

The CBH approach can be applied to adsorbates on metal oxide surfaces in the same way as for transition-metal facets, without any modifications. We focus on MgO(100) in this study due to the amount of experimental data that is available in the literature.[15] Experimental adsorption enthalpies on MgO(100) are currently limited to physisorbed species, including CH$_4$, C$_2$H$_6$, C$_3$H$_8$, n-C$_4$H$_{10}$, n-hexane, and n-octane.[12,58] With this set of species, it is possible to derive error-cancellation reactions for all physisorbed n-alkanes larger than ethane. A schematic of the hierarchy of error cancellation reactions for adsorbed n-hexane on MgO(100) is provided in Fig. 4a. The bond-separation reaction (CBH-1) contains only C–C bonds, for which C$_2$H$_6^*$ is used as the reference species in combination with CH$_4^*$
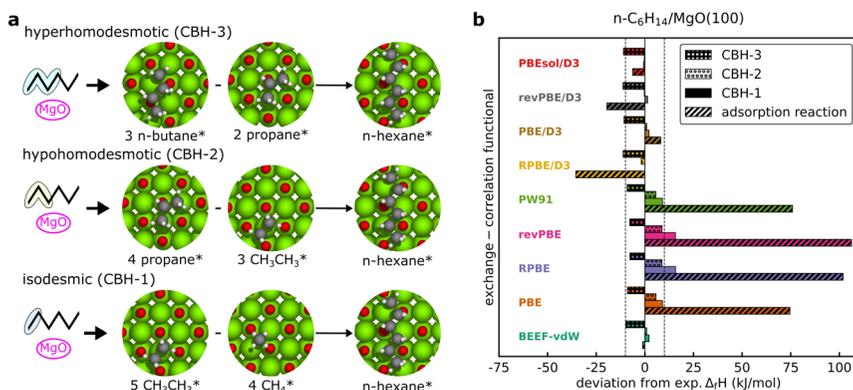

Fig. 4 (a) CBH reaction scheme for n-hexane adsorbed on MgO(100) and (b) deviation of the n-C$_6$H$_{14}^*$ enthalpies of formation derived via the CBH scheme and adsorption reaction from the experimental value. The colored area in the Lewis structure indicates the conserved fragments at the different CBH rungs.

to balance the stoichiometry. At the CBH-2 level, the C–C–C chain is conserved and the C–C–C–C backbone at the CBH-3 level, requiring $C_3H_8^*$ and n-$C_4H_{10}^*$ as reference species. Reference species that are products at lower rungs become the reactants at the higher rungs.[36] The total number of reference species decreases when climbing the CBH rungs since larger fragments are conserved; 9 references at CBH-1, 7 at CBH-2, and 5 at CBH-3. Any uncertainties in the experimental values are thus multiplied, which can significantly affect the lower rungs.[38] Higher rungs have a higher degree of error cancellation in combination with fewer references and are thus supposedly more accurate.[36,41,42] The referencing reactions for the other n-alkanes are summarized in the SI.

Similar to the benchmarking of the enthalpies of formation of adsorbates on transition metal surfaces, we compared the conventional adsorption reaction and error-cancellation method with experimental values for physisorbed n-alkanes on MgO(100). Fig. 4b shows the results for n-hexane, and the results for the other species are reported in Fig. S2. The trends for the MgO(100) surface are similar to the results of the physisorbed alkanes on Pt(111) (see Fig. 2a). Values derived via the adsorption reaction approach using the BEEF-vdW functional yield a good agreement with the experiments. The functionals with added D3 dispersion correction also perform well for the smaller alkanes, but deviations increase for larger alkanes, as seen for n-hexane. Enthalpies of formation from the RPBE, PBE, or PW91 functional deviate by more than 70 kJ mol^{-1} for n-hexane, while the deviation is larger than 150 kJ mol^{-1} for n-octane. Using the error-cancellation reactions improves the accuracy of the derived enthalpy of formation for all exchange–correlation functionals. The largest deviation at the CBH-1 level occurs for RPBE and revPBE without dispersion corrections. Still, these differ only by 15 kJ mol^{-1} from the experiment instead of 100 kJ mol^{-1} compared to the conventional approach. Climbing to CBH-2 leads to increasingly more accurate enthalpies of formation. All values are within the experimental uncertainty. There is an increase in the deviation from experiment at the CBH-3 level, where all functionals predict more negative enthalpies of formation for n-hexane at the CBH-3 rung.

The adsorbates were optimized with the BEEF-vdW functional in this study, and only single-point energy calculations for this optimized configuration were performed with the other functionals. We performed additional relaxations for propane and n-butane on MgO(100) with the PBE functional to investigate the implications of this simplification. The enthalpies of formation of the optimized structure exhibit only minor differences for all methods (see Fig. S3) and do not change the conclusions that can be drawn from this work.

We also performed the uncertainty quantification using the error estimates of the BEEF ensembles for the adsorbates on MgO(100), which is shown in Fig. 5. Enthalpies of formation for propane determined from the isodesmic reaction are all within an astonishing 1 kJ mol^{-1} regardless of the exchange–correlation functional. The standard deviation spanned by the BEEF functional is reduced by more than a factor of 17 compared to the conventional approach. The enthalpy of the isodesmic reaction is only 7 kJ mol^{-1}, which also highlights an excellent error cancellation. Results for n-butane are equally good. The uncertainty is reduced by a factor of 10 using an isodesmic reaction, and all functionals predict enthalpies of formation to within 2 kJ mol^{-1}. The CBH-2 level performs even better, and all results are tightly clustered around the experimental value with a standard
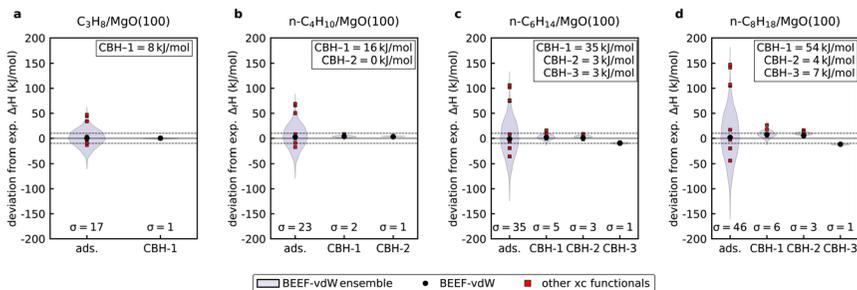
Fig. 5 Benchmarking of the adsorption reaction and CBH method for physisorbed (a) $C_3H_8^*$, (b) $n\text{-}C_4H_{10}^*$, (c) $n\text{-}C_6H_{14}^*$, and (d) $n\text{-}C_8H_{18}^*$ on MgO(100). Only CBH-1 is possible for $C_3H_8^*$ and CBH-2 is the highest rung for $n\text{-}C_4H_{10}^*$, whereas CBH-3 can be used for n-hexane and n-octane. The contour shows the uncertainty spanned by the BEEF ensemble.

deviation for the BEEF ensemble of 1 kJ mol^{-1}. Evaluating the results for n-hexane and n-octane reveals similar trends. The error cancellation led to significant reductions in the uncertainty compared to the adsorption reaction approach from 5 kJ mol^{-1} (CBH-1) to 3 kJ mol^{-1} (CBH-2) and finally 1 kJ mol^{-1} (CBH-3).

The increase in uncertainty for the conventional adsorption reaction approach with increasing alkane size, and to a much lesser extent for the CBH reactions, can be explained by the increasing number of reference species required to balance the stoichiometry. This fact especially highlights the shortcomings of the conventional approach. More reference species are required for the larger alkenes, leading to a compounding of errors.[38] However, the enthalpies of formation predicted by the nominal BEEF-vdW value are still in good agreement with the experiments, but other functionals deviate by up to 150 kJ mol^{-1} for n-octane. Furthermore, it is not guaranteed that the experimental value is within the BEEF-vdW uncertainty range.[46] The isodesmic reactions cancel out most errors for the larger alkanes, leading to accurate predictions within the uncertainty range. Results at the CBH-1 and CBH-2 levels are in good agreement with the experimental results for all species. However, CBH-3 predicts more negative enthalpies of formation than observed experimentally for n-hexane and n-octane. This consistent deviation from the experiments could point to coverage effects in the experimental results, since the larger alkanes cover more sites on the catalyst's surface and could exhibit repulsive interactions as seen for $n\text{-}C_4H_{10}^*$ on Pt(111). The experimental enthalpies of formation are derived from TPD experiments, and the exact coverage for the evaluated desorption enthalpy cannot be accurately determined. Additionally, the experimental enthalpies of formation are also subject to uncertainties. A consistent shift at the CBH-3 level could point to an error in the experimental enthalpy of formation of butane. All experimental enthalpies of formation for the alkanes were derived by Tait and co-workers,[12,58] but only butane was determined in a different study, which could explain the offset.[58]

Discussion

The usage of the modified CBH framework allows the automated construction of error-cancellation reactions for adsorbates on metal and metal oxide surfaces. In combination with the known enthalpies of formation of the reference species (here from surface science experiments), this approach can be used to derive the enthalpies of formation of adsorbates from GGA-DFT data with beyond-DFT accuracy. Accurate thermophysical properties of intermediates are crucial for accurate predictions from detailed chemical kinetic models since the catalytic activity is not just controlled by reaction kinetics.[60,61] The error-cancellation approach can only be applied to determine the thermophysical properties of adsorbed species and is not a method to compute the activation barriers of elementary reactions. Activation barriers are calculated from the energy difference of the transition and initial state, which can have some degree of error cancellation due to the structural similarity.

Currently, the bottleneck for the widespread application of this method for other catalytic surfaces is the limited availability of highly accurate reference enthalpies of formation of adsorbates. There is only enough experimental surface science data to construct these error-cancellation reactions for Pt(111) and to some extent for Ni(111) and only for $C_xH_yO_z$ adsorbates.[13–15] The amount of highly accurate enthalpies of formation derived from higher level of theory electronic structure methods is even further limited. A major advantage of the CBH method is that it not only improves the accuracy of thermophysical properties but also identifies the set of reference species for which highly accurate enthalpies of formation are required. In order to construct isodesmic reactions, which already have significantly improved the accuracy over the conventional approach, only 10 reference species are required to capture all the bond types of $C_xH_yO_z$ adsorbates.[43] For a microkinetic model for the conversion of hydrocarbons, e.g. Fischer–Tropsch synthesis, it would thus only be necessary to perform 10 highly accurate calculations via RPA[18,19] or quantum Monte Carlo[22] for the catalytic surface of interest. The rest of the species can be computed via GGA-DFT, which is feasible with the current computational resources. The CBH method can be used with every electronic structure method to map a lower level of theory to a higher level of theory through error cancellation, which has been demonstrated in many studies in the gas-phase community.[37,38] More reference species are required to climb to the higher rungs or to incorporate other heteroatoms (e.g. N). The CBH method can also be applied to complex catalytic surfaces and facets, including multi-metallic surfaces, mixed metal oxides, or restructured surfaces. The only requirement for the application of the structure-based decomposition in the CBH approach is a Lewis structure of the target. Typically, this structure can be easily deduced from an optimized geometry. In rare cases, more complex electronic configurations can occur in the target species such as resonance,[43,62] which requires further development of the CBH method.

In this study, we integrated available experimental data from surface science with electronic structure theory rather than simply benchmarking computational results for adsorbates. Thus, the CBH method provides an easy way to connect various levels of theory, gas-phase thermochemical data, and surface science data into a single global thermochemical network,[9] which provides a step towards the

construction of global thermochemical databases for adsorbates. The integration of data from various sources also poses a hurdle in the construction of foundational machine learning models for heterogeneous systems.[63] This hurdle can be overcome through the framework of these error-cancellation reactions. We would also like to emphasize that the concept of error-cancellation reactions is distinctly different from group-additivity methods,[64,65] which can also be used to determine thermochemical properties of adsorbates. The structure-based fragmentation of the target species is similar for both approaches, but the CBH method calculates the enthalpy of formation from actual electronic structure data, whereas group additivity computes the enthalpy of formation as a sum of the enthalpy contributions of the fragments. It is possible to train group-additivity methods on the accurate enthalpies of formation derived from the CBH approach.

While the CBH method can yield highly accurate enthalpies of formation, this is not guaranteed, as seen for formic acid and monodentate formate on Pt(111). Especially at the lower rungs, hybridization of the species is not necessarily conserved, which can result in poor performance of the CBH reaction. Chan and co-workers[51,52] showed that handcrafted reactions based on chemical intuition can sometimes outperform the systematic CBH method for molecular systems. However, the concept of using error-cancellation reactions to accurately determine the enthalpies of formation of adsorbates represents a new direction for the field of computational catalysis.

Conclusions

In this work, we demonstrated the usage of error cancellation reactions using the connectivity-based hierarchy to derive enthalpies of formation of adsorbates that move beyond the limitations of the accuracy of DFT with GGA exchange–correlation functionals. The CBH method is universally applicable, and we have demonstrated the applicability for chemi- and physisorbed species on Pt(111) and Ni(111). Additionally, the method was successfully used to derive accurate enthalpies of formation of *n*-alkanes on MgO(100). It was possible to derive enthalpies of formation for up to *n*-octane to within experimental accuracy from DFT with GGA exchange–correlation functionals. Error-cancellation reactions drastically reduce the differences between GGA exchange–correlation functionals, thereby overcoming the challenge of selecting the best functional. The combination of CBH with uncertainty quantification using the error estimates of the BEEF-vdW functional clearly demonstrates the effectiveness of this method and provides a means to assess performance in the absence of accurate benchmark data. Using experimental surface science data, combined with error-cancellation reactions, leads to more accurate thermophysical properties of adsorbates, with far-reaching implications for more predictive multiscale modeling of heterogeneously catalyzed reactions.

Author contributions

S. G. P.: data curation, formal analysis, writing – original draft; B. K.: conceptualization, funding acquisition, data curation, formal analysis, investigation, software, writing – original draft, writing – review & editing.

Conflicts of interest

There are no conflicts to declare.

Data availability

Data for this article, including DFT data and scripts are available on Zenodo at https://doi.org/10.5281/zenodo.17787002.

Supplementary information (SI): raw DFT data, optimized structures, additional results for MgO(100). See DOI: https://doi.org/10.1039/d5fd00144g.

Acknowledgements

Notes and references

1 M. Salciccioli, M. Stamatakis, S. Caratzoulas and D. Vlachos, *Chem. Eng. Sci.*, 2011, **66**, 4319–4355.

2 K. Blöndal, K. Sargsyan, D. H. Bross, B. Ruscic and C. F. Goldsmith, *ACS Catal.*, 2023, **13**, 19–32.

3 L. H. Sprowl, C. T. Campbell and L. Árnadóttir, *J. Phys. Chem. C*, 2016, **120**, 9719–9731.

4 B. Ruscic, R. E. Pinzon, G. von Laszewski, D. Kodeboyina, A. Burcat, D. Leahy, D. Montoy and A. F. Wagner, *J. Phys.:Conf. Ser.*, 2005, **16**, 561–570.

5 B. Ruscic and D. H. Bross, Active Thermochemical Tables (ATcT) Values Based on ver. 1.220 of the Thermochemical Network, https://atct.anl.gov, (accessed 2025-11-01).

6 A. Karton, E. Rabinovich, J. M. L. Martin and B. Ruscic, *J. Chem. Phys.*, 2006, **125**, 144108.

7 S. J. Klippenstein, L. B. Harding and B. Ruscic, *J. Phys. Chem. A*, 2017, **121**, 6580–6602.

8 M. E. Harding, J. Vázquez, B. Ruscic, A. K. Wilson, J. Gauss and J. F. Stanton, *J. Chem. Phys.*, 2008, **128**, 114111.

9 B. Kreitz, G. S. Gusmão, D. Nai, S. J. Sahoo, A. A. Peterson, D. H. Bross, C. F. Goldsmith and A. J. Medford, *Chem. Soc. Rev.*, 2025, **54**, 560–589.

10 C. T. Campbell, *Acc. Chem. Res.*, 2019, **52**, 984–993.

11 W. A. Brown, R. Kose and D. A. King, *Chem. Rev.*, 1998, **98**, 797–832.

12 S. L. Tait, Z. Dohnálek, C. T. Campbell and B. D. Kay, *J. Chem. Phys.*, 2005, **122**, 164708.

13 T. L. Silbaugh and C. T. Campbell, *J. Phys. Chem. C*, 2016, **120**, 25161–25172.

14 C. T. Campbell, J. Fingerhut and A. M. Wodtke, *Surf. Sci.*, 2025, **756**, 122714.

15 C. T. Campbell and J. R. V. Sellers, *Chem. Rev.*, 2013, **113**, 4106–4135.

16 T. Avanesian, S. Dai, M. J. Kale, G. W. Graham, X. Pan and P. Christopher, *J. Am. Chem. Soc.*, 2017, **139**, 4551–4558.

17 R. B. Araujo, G. L. S. Rodrigues, E. C. dos Santos and L. G. M. Pettersson, *Nat. Commun.*, 2022, **13**, 6853.

18 N. A. Szaro, M. Bello, C. H. Fricke, O. H. Bamidele and A. Heyden, *J. Phys. Chem. Lett.*, 2023, **14**, 10769–10778.

19 H. Kim, N.-K. Yu, N. Tian and A. J. Medford, *J. Phys. Chem. C*, 2024, **128**, 11159–11175.

20 C. Sheldon, J. Paier and J. Sauer, *J. Chem. Phys.*, 2021, **155**, 174702.

21 B. T. G. Lau, G. Knizia and T. C. Berkelbach, *J. Phys. Chem. Lett.*, 2021, **12**, 1104–1109.

22 G. R. Iyer and B. M. Rubenstein, *J. Phys. Chem. A*, 2022, **126**, 4636–4646.

23 Q. Zhao and E. A. Carter, *J. Chem. Theory Comput.*, 2020, **16**, 6528–6538.

24 J. Wellendorff, T. L. Silbaugh, D. Garcia-Pintos, J. K. Nørskov, T. Bligaard, F. Studt and C. T. Campbell, *Surf. Sci.*, 2015, **640**, 36–44.

25 E. Romeo, F. You, H. Ma, F. Illas, B. S. Yeo and F. Calle-Vallejo, *ACS Catal.*, 2025, **15**, 18004–18012.

26 A. A. Peterson, F. Abild-Pedersen, F. Studt, J. Rossmeisl and J. K. Nørskov, *Energy Environ. Sci.*, 2010, **3**, 1311.

27 R. Christensen, H. A. Hansen and T. Vegge, *Catal. Sci. Technol.*, 2015, **5**, 4946–4949.

28 B. Kreitz, G. D. Wehinger, C. F. Goldsmith and T. Turek, *ChemCatChem*, 2022, **14**, e202200570.

29 A. J. Medford, J. Wellendorff, A. Vojvodic, F. Studt, F. Abild-Pedersen, K. W. Jacobsen, T. Bligaard and J. K. Nørskov, *Science*, 2014, **345**, 197–200.

30 B. Kreitz, P. Lott, F. Studt, A. J. Medford, O. Deutschmann and C. F. Goldsmith, *Angew. Chem., Int. Ed.*, 2023, **62**, e202306514.

31 E. A. Walker, D. Mitchell, G. A. Terejanu and A. Heyden, *ACS Catal.*, 2018, **8**, 3990–3998.

32 B. Kreitz, G. Kogekar, R. Cheula and C. F. Goldsmith, *J. Catal.*, 2025, **452**, 116407.

33 J. A. Pople, L. Radom and W. J. Hehre, *J. Am. Chem. Soc.*, 1971, **93**, 289–300.

34 W. J. Hehre, R. Ditchfield, L. Radom and J. A. Pople, *J. Am. Chem. Soc.*, 1970, **92**, 4796–4801.

35 S. E. Wheeler, K. N. Houk, P. v. R. Schleyer and W. D. Allen, *J. Am. Chem. Soc.*, 2009, **131**, 2547–2560.

36 R. O. Ramabhadran and K. Raghavachari, *J. Chem. Theory Comput.*, 2011, **7**, 2094–2103.

37 B. Chan, E. Collins and K. Raghavachari, *WIREs: Comput. Mol. Sci.*, 2021, **11**, e1501.

38 S. E. Wheeler, *WIREs: Comput. Mol. Sci.*, 2012, **2**, 204–220.

39 A. Sengupta, R. O. Ramabhadran and K. Raghavachari, *J. Comput. Chem.*, 2016, **37**, 286–295.

40 A. Sengupta and K. Raghavachari, *J. Chem. Theory Comput.*, 2014, **10**, 4342–4350.

41 S. N. Elliott, M. Keçeli, M. K. Ghosh, K. P. Somers, H. J. Curran and S. J. Klippenstein, *J. Phys. Chem. A*, 2023, **127**, 1512–1531.

42 K. Abeywardane and C. F. Goldsmith, *ACS Phys. Chem. Au*, 2024, **4**, 247–258.

43 B. Kreitz, K. Abeywardane and C. F. Goldsmith, *J. Chem. Theory Comput.*, 2023, **19**, 4149–4162.

44 P. Giannozzi, O. Baseggio, P. Bonfà, D. Brunato, R. Car, I. Carnimeo, C. Cavazzoni, S. de Gironcoli, P. Delugas, F. Ferrari Ruffino, A. Ferretti, N. Marzari, I. Timrov, A. Urru and S. Baroni, *J. Chem. Phys.*, 2020, **152**, 154105.

45 P. Giannozzi, S. Baroni, N. Bonini, M. Calandra, R. Car, C. Cavazzoni, D. Ceresoli, G. L. Chiarotti, M. Cococcioni, I. Dabo, A. Dal Corso, S. de Gironcoli, S. Fabris, G. Fratesi, R. Gebauer, U. Gerstmann, C. Gougoussis, A. Kokalj, M. Lazzeri, L. Martin-Samos, N. Marzari, F. Mauri, R. Mazzarello, S. Paolini, A. Pasquarello, L. Paulatto, C. Sbraccia, S. Scandolo, G. Sclauzero, A. P. Seitsonen, A. Smogunov, P. Umari and R. M. Wentzcovitch, *J. Phys.:Condens. Matter*, 2009, **21**, 395502.

46 J. Wellendorff, K. T. Lundgaard, A. Møgelhøj, V. Petzold, D. D. Landis, J. K. Nørskov, T. Bligaard and K. W. Jacobsen, *Phys. Rev. B*, 2012, **85**, 235149.

47 S. Grimme, J. Antony, S. Ehrlich and H. Krieg, *J. Chem. Phys.*, 2010, **132**, 154104.

48 K. Blondal, J. Jelic, E. Mazeau, F. Studt, R. H. West and C. F. Goldsmith, *Ind. Eng. Chem. Res.*, 2019, **58**, 17682–17691.

49 V. Vorotnikov, S. Wang and D. G. Vlachos, *Ind. Eng. Chem. Res.*, 2014, **53**, 11929–11938.

50 E. M. Collins, A. Sengupta, D. I. AbuSalim and K. Raghavachari, *J. Phys. Chem. A*, 2018, **122**, 1807–1812.

51 B. Chan, Y. Kawashima, M. Katouda, T. Nakajima and K. Hirao, *J. Am. Chem. Soc.*, 2016, **138**, 1420–1429.

52 B. Chan and A. Karton, *Phys. Chem. Chem. Phys.*, 2021, **23**, 17713–17723.

53 E. M. Karp, T. L. Silbaugh, M. C. Crowe and C. T. Campbell, *J. Am. Chem. Soc.*, 2012, **134**, 20388–20395.

54 S. J. Carey, W. Zhao, E. Harman, A.-K. Baumann, Z. Mao, W. Zhang and C. T. Campbell, *ACS Catal.*, 2018, **8**, 10089–10095.

55 S. L. Tait, Z. Dohnálek, C. T. Campbell and B. D. Kay, *J. Chem. Phys.*, 2006, **125**, 234308.

56 T. L. Silbaugh, E. M. Karp and C. T. Campbell, *J. Am. Chem. Soc.*, 2014, **136**, 3964–3971.

57 W. Zhao, S. J. Carey, Z. Mao and C. T. Campbell, *ACS Catal.*, 2018, **8**, 1485–1489.

58 S. L. Tait, Z. Dohnálek, C. T. Campbell and B. D. Kay, *J. Chem. Phys.*, 2005, **122**, 164707.

59 S. G. Porter and B. Kreitz, Data for Thermophysical Properties of Adsorbates with Beyond-DFT Accuracy from DFT Data through Error Cancellation, *Zenodo*, 2025, DOI: 10.5281/zenodo.17787002.

60 G. Pio, X. Dong, E. Salzano and W. H. Green, *Combust. Flame*, 2022, **241**, 112080.

61 J. E. Sutton, W. Guo, M. A. Katsoulakis and D. G. Vlachos, *Nat. Chem.*, 2016, **8**, 331–337.

62 A. Grinberg Dana, M. Liu and W. H. Green, *Int. J. Chem. Kinet.*, 2019, **51**, 760–776.

63 B. M. Wood, M. Dzamba, X. Fu, M. Gao, M. Shuaibi, L. Barroso-Luque, K. Abdelmaqsoud, V. Gharakhanyan, J. R. Kitchin, D. S. Levine, K. Michel, A. Sriram, T. Cohen, A. Das, A. Rizvi, S. J. Sahoo, Z. W. Ulissi and C. L. Zitnick, UMA: A Family of Universal Models for Atoms, *arXiv*, 2025, preprint, arXiv:2506.23971, DOI: 10.48550/arXiv.2506.23971.

64 G. R. Wittreich and D. G. Vlachos, *Comput. Phys. Commun.*, 2022, **273**, 108277.

65 M. Salciccioli, Y. Chen and D. G. Vlachos, *J. Phys. Chem. C*, 2010, **114**, 20155–20166.